Available online at www.worldscientificnews.com

World Scientific News

WSN 40 (2016) 264-283 EISSN 2392-2192

Electron dynamics in a strong laser field with Gaussian Potential well

C. C. Gunatilaka, K. A. I. L. Wijewardena Gamalath*

Department of Physics, University of Colombo, Colombo 3, Sri Lanka

*E-mail address: imalie@phys.cmb.ac.lk

ABSTRACT

The time dependant Schrodinger equation was solved for one dimensional and two dimensional Gaussian potential wells in the presence of a strong laser field. Three laser fields Argon, Helium-Neon and Ti-Sapphire with different intensities with cosine and sine laser electric fields were used for the simulation. The Gaussian potential well get distorted in two different ways with the intensity change and the wavelength change of the laser. The wave functions and the position probabilities are presented. The Gaussian potential distortion for He-Ne laser occur in the opposite way compared to Ar and Ti-Sapphire for cosine electric field while Ar laser behaves differently than He-Ne and Ti-Sapphire for sine electric field of the laser in the case of two dimensional potential.

***Keywords*:** Strong laser field; Gaussian potential well; Argon, Helium-Neon; Ti-Sapphire; time dependant Schrodinger equation

1. INTRODUCTION

When a high power laser is focused into a gas of atoms, the atomic potential gets distorted reducing the potential barrier and the electrons have a possibility to tunnel through the reduced barrier [1]. When an intense laser beam is directed into a gas or solid, and the electric field of the laser beam is comparable with that of the atoms, the high harmonic generation occurs. High harmonic generation can be discussed using the three step model and

it is an important concept to study the electron dynamics in a strong laser field. The three steps are laser ionization, propagation and recombination. The laser ionization and the recombination are quantum mechanical processes and electron propagation can be treated as a classical process [2]. In 2001 two teams independently demonstrated that high harmonic generation led to the emission of ultra-short light bursts, lasting just a few hundred attoseconds. This sparked the emergence of the new field of attosecond science [3]. When an electron was ejected from the parent atom, as the laser changes the direction, the electron accelerated back and re-collided with the parent ion [1]. When the electron re-collides with the parent iron, three possibilities can be occurred.

The electrons scatter elastically, in elastically and recombined with the parent iron emitting energy of photons. Harmonics can be seen only in the third possibility and the produced high order harmonics propagated collinearly with the laser field. In the harmonic spectrum only the odd multiples were seen and there were three regions that can be identified with the characteristics of the spectrum. The three regions were perturbative, plateau and cut-off as shown in Figure 1 [2]. The intensity of the peaks had dropped rapidly in the first few harmonics and it was because the efficiency of the process had decreased with the order. In the plateau region most of the peaks have the same intensity and it cannot be explained from the three step model. After that there was a sudden cut-off. This whole process was periodic [2].

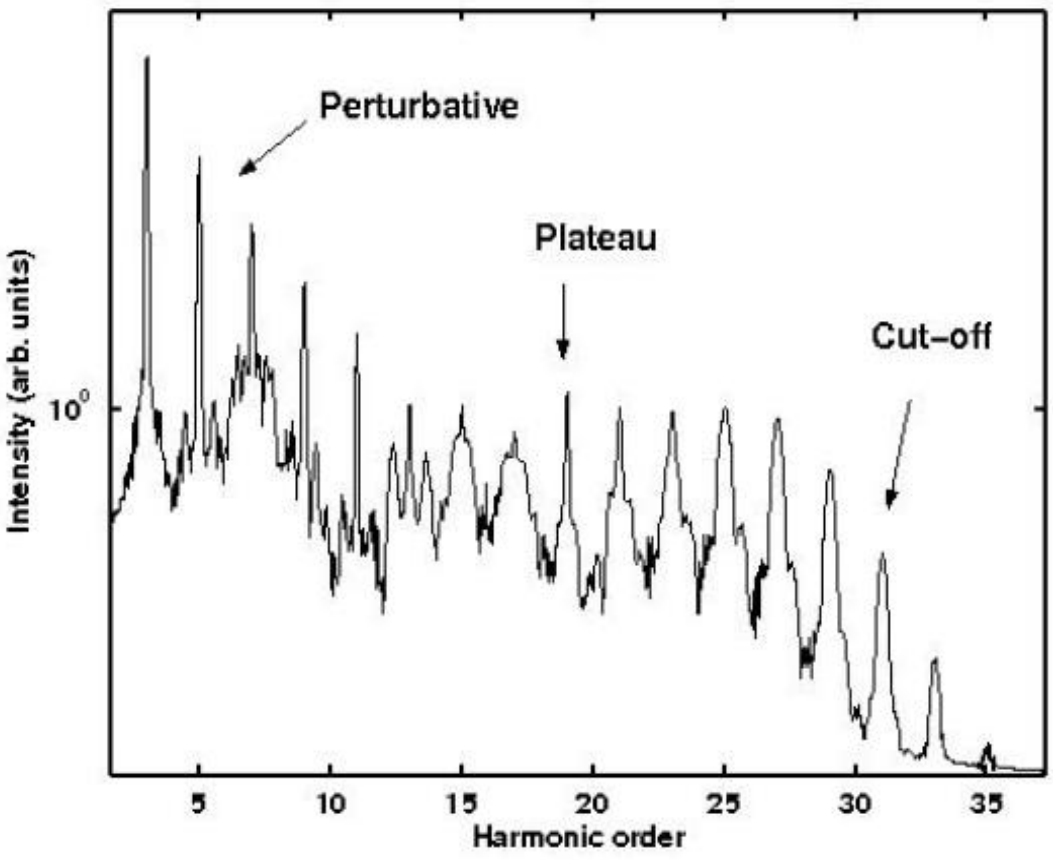

Figure 1. Harmonic spectrum of Argon using a laser peak intensity of 1.4×10^{18} Wm^{-2} [2].

Theorists have concentrated their effort on solving Schrodinger equation for the hydrogen atom, a single active electron atom in a strong laser filed. A number of methods have been proposed to solve this problem but two methods, the three step model and the strong field approximation method stand out [2]. Lewenstein developed a model called the Lewenstein model for the quantum theory of high harmonic generation in order to solve the time dependant Schrodinger equation based on several assumptions mainly the strong field approximation assumption [4]. Forth order Runge-Kutta method was also used to solve the time dependant Schrodinger equation but not for the case when a system is distorted due a strong laser field due to its complexity. To solve the time dependant Schrodinger equation using the computer software, Split step method was widely used due to the straight forward simulation steps [5].

In a previous work, the three step model of high harmonic generation was used to investigate the electron behaviour in strong laser fields of Argon, Helium-Neon and Ti-Sapphire [6]. In this paper this work has been extended to simulate the dynamics of an electron in an atomic potential in the presence of a strong laser field by solving the time dependent Schrodinger equation numerically. The Gaussian potential well was analyzed using different laser wavelengths, 500 nm, 632.8 nm and 800 nm lasers and intensities $1.6\times10^{18}\,\mathrm{Wm^{-2}}$, $5\times10^{18}\,\mathrm{Wm^{-2}}$ and $40\times10^{18}\,\mathrm{Wm^{-2}}$. The time dependant Schrodinger equation was solved for the system of single electron in a hydrogen atom using the one dimensional and two dimensional Gaussian atomic potential well with the application of strong external cosine and sine laser electric fields. The wave functions and position probability densities are also presented for sine and cosine laser electric fileds for the intensity $5\times10^{18}\,\mathrm{Wm^{-2}}$.

2. ONE DIMENSIONAL GAUSSIAN WELL

When a strong laser field is applied to an atomic potential, the shape of the atomic potential changes and the electrons will have a higher tunnelling probability compared to the atomic potential without an external laser field. Time dependent Schrodinger equation with an external laser field [4] in the x-direction:

$$\frac{-\hbar^2}{2m}\frac{\partial^2\Psi(x,t)}{\partial x^2}+V(x)Z(x,t)+xE(t)\Psi(x,t)\;=\;i\hbar\frac{\partial\Psi(x,t)}{\partial t} \qquad (1)$$

where m is the mass of the electron, and $\Psi(x,t)$ is the time dependent wave function, $V(x)$ is the atomic potential. A Gaussian potential well can be represented as,

$$V(x)\;=\;-V_0e^{-\alpha x^2}\;\;(\alpha>0,\;V_0>0;\;-\infty\le x\le+\infty)\;. \qquad (2)$$

Equation 1 with Gaussian potential well was solved by Split step method using the Matlab software. Simulations were done using the initial condition that the atomic potential was without an external laser field for a hydrogen atom with the single electron. The wave function of the Schrodinger equation for the Gaussian potential well is [7],

$$\Psi(x,t) = \left(\frac{2b}{\pi}\right)^{\frac{1}{4}} e^{-bx^2} e^{\frac{-iEt}{\hbar}} \qquad (3)$$

b is related to the width of the potential well and the energy eigenvalue *E* is given by

$$E = \left(\frac{-\hbar^2}{2m}\right)\left(4x^2b^2 - 2b\right) + V_0(x) \qquad (4)$$

Simulations were carried out using the two different laser fields, cosine electric field $E_0\cos(\omega_0 t)$ and the sine electric field $E_0\sin(\omega_0 t)$ with different wavelengths namely, Ar laser with 500 nm, He-Ne laser with 632.8 nm and Ti-Sapphire laser with 800 nm with intensities $1.6\times10^{18}\,\mathrm{Wm^{-2}}$, $5\times10^{18}\,\mathrm{Wm^{-2}}$ and $40\times10^{18}\,\mathrm{Wm^{-2}}$. The Gaussian potential well used for simulation is shown in Figure 2. The ionization energy of the ground state electron was chosen as the depth of the Gaussian potential well and the values were measured in atomic units. Ionization energy of 13.6 eV was used in atomic units in the simulations for a single electron process.

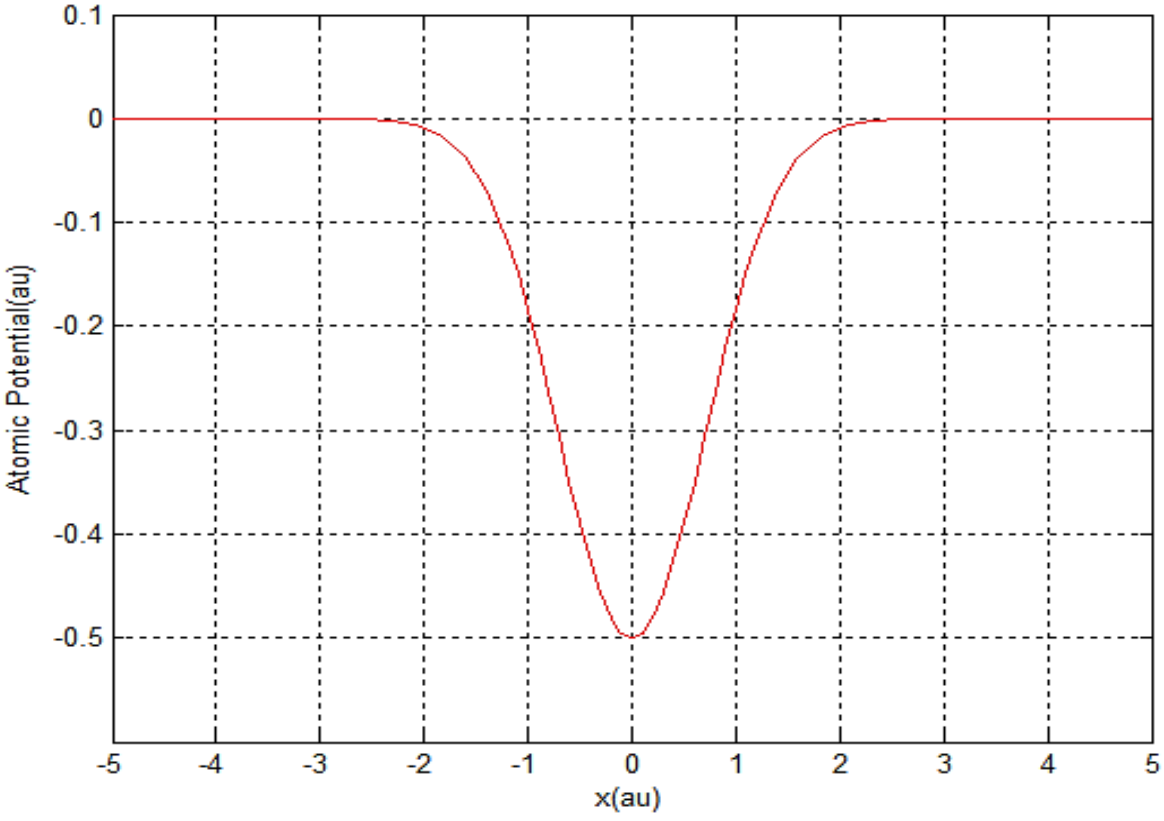

Figure 2. Gaussian potential well used for simulation.

3. COSINE LASER ELECTRIC FIELD

The distortions of the atomic potential due to the presence of a strong Ar laser with a cosine electric with different intensities are shown in Figure 3. Black color data points represent the Gaussian potential well without an external laser field. Blue, red and green lines represent the distorted Gaussian potential after applying the Ar laser intensities of $40\times10^{18}\,\mathrm{Wm}^{-2}$, $5\times10^{18}\,\mathrm{Wm}^{-2}$ and $1.6\times10^{18}\,\mathrm{Wm}^{-2}$ respectively. When the laser intensity increases, the tunnelling probability increases. Figure 4 shows the distortion of the Gaussian potential due three different lasers, Ar laser λ = 500 nm in green, He-Ne laser λ = 632.8 nm nm in red and Ti-Sapphire laser λ = 800 nm in blue with cosine electric field intensity of $5\times10^{18}\,\mathrm{Wm}^{-2}$. Black colour data points represent the Gaussian potential well without an external laser field. The Gaussian barrier is reduce in the negative direction of *x*-axis for Ar laser and Ti-Sapphire laser, but for the He-Ne laser, the Gaussian barrier reduction occurs in the positive direction of the *x*-axis.

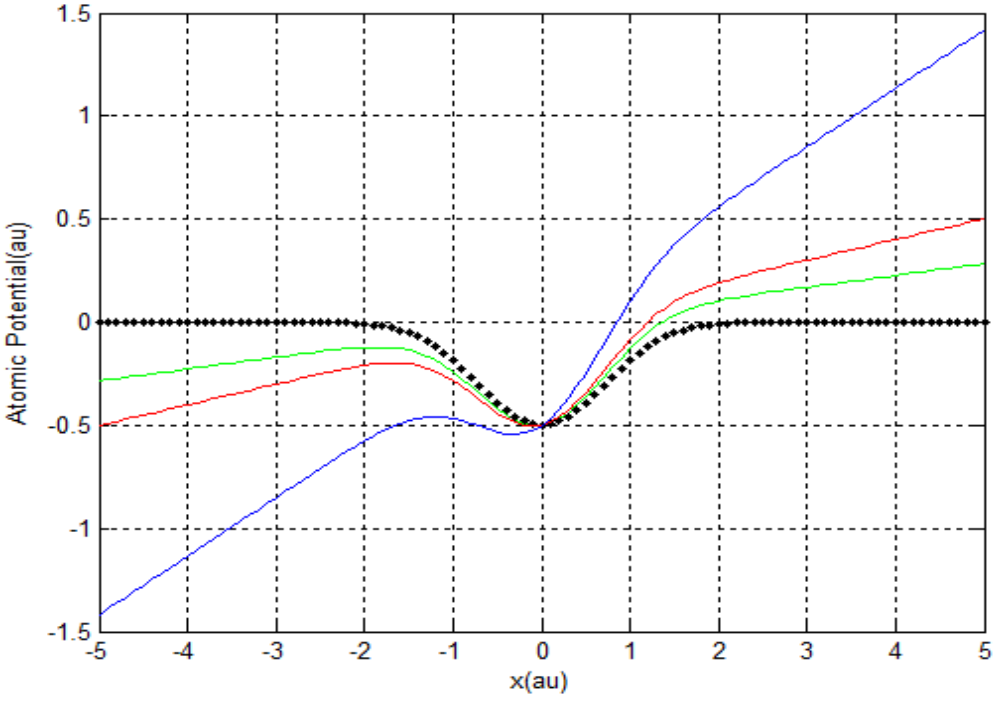

Figure 3. Atomic potential distortion due to the Ar laser field with different cosine electric field intensities. Blue, red and green lines represent the intensities, $40\times10^{18}\,\mathrm{Wm}^{-2}$, $5\times10^{18}\,\mathrm{Wm}^{-2}$ and $1.6\times10^{18}\,\mathrm{Wm}^{-2}$. Black lines are without an external laser field.

The wave function and the position probability density of the Ar, He-Ne and Ti-Sapphire laser fields with different intensities for the cosine electric field is shown in Figure 5 and 6 respectively. Red, blue and black colour lines represents laser field intensity of 1.6×10^{18}, 5×10^{18} and $40\times10^{18}\,\mathrm{Wm}^{-2}$.

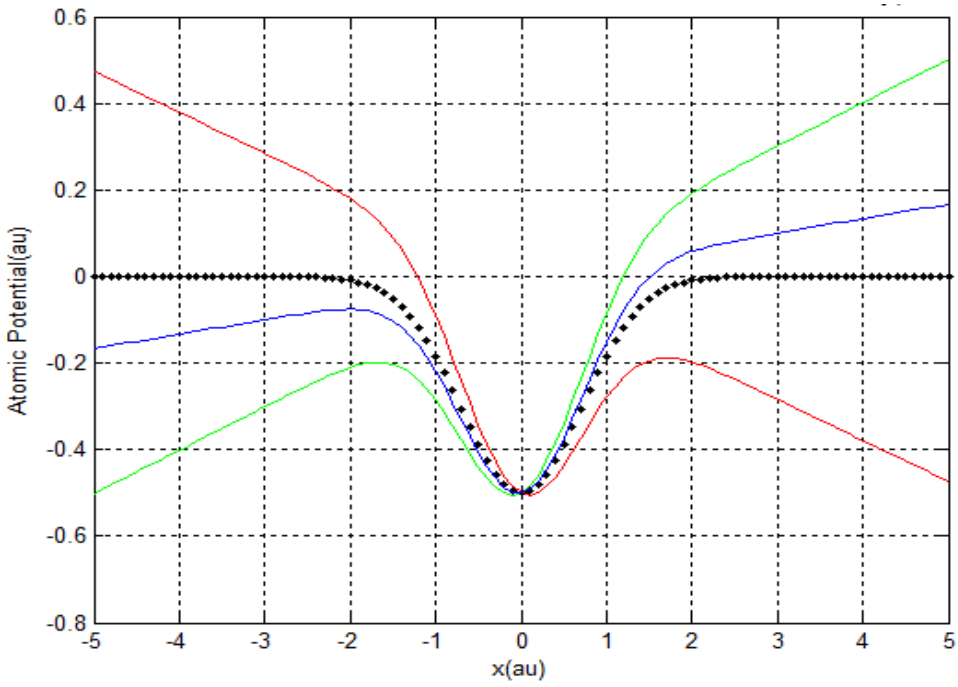

Figure 4. Atomic potential distortion due to cosine electric field intensity of $5\times10^{18}\,\mathrm{Wm}^{-2}$. Green red and blue, lines represent Ar, He-Ne and Ti-sapphire laser. Black lines are without an external laser field.

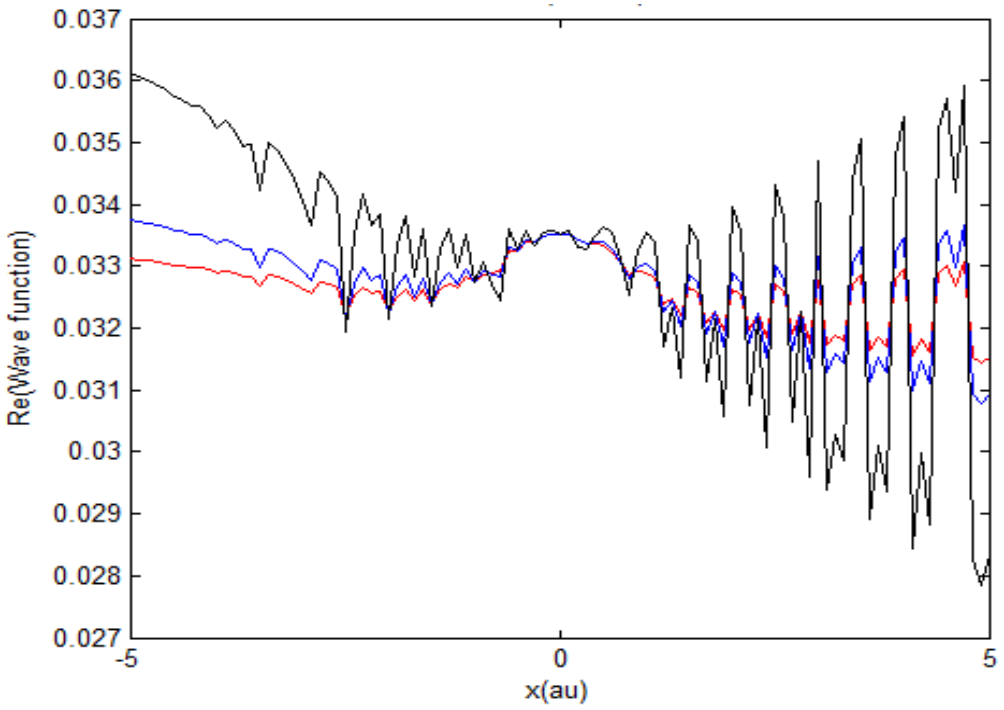

Figure 5(a). Wave function for Ar laser with different intensities $1.6\times10^{18}\,\mathrm{Wm}^{-2}$ (red), $5\times10^{18}\,\mathrm{Wm}^{-2}$ (blue) and $40\times10^{18}\,\mathrm{Wm}^{-2}$ (black) for cosine laser electric field.

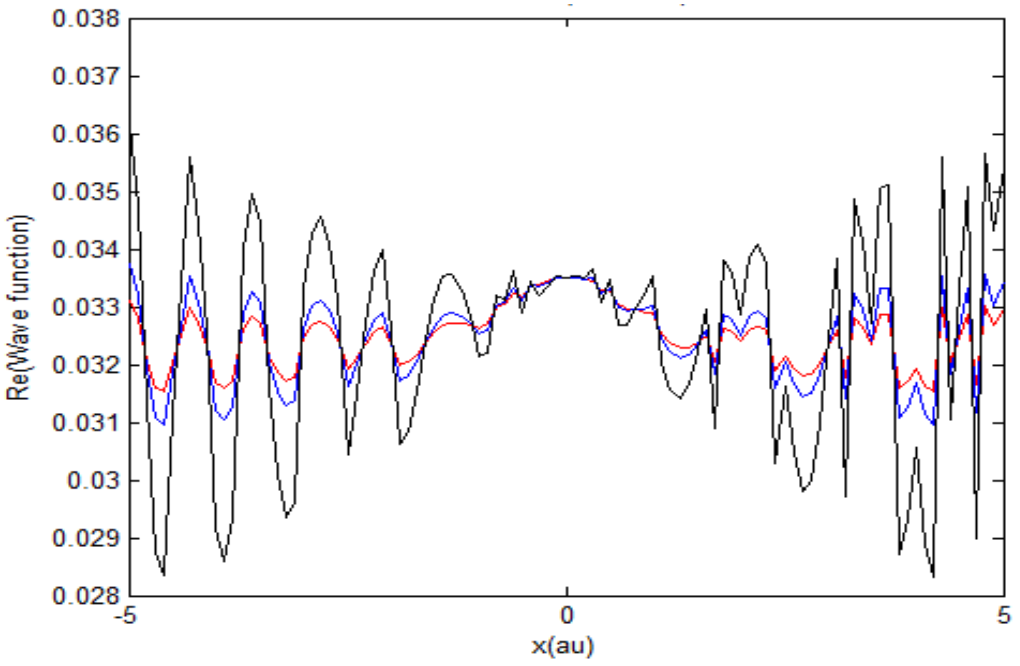

5(*b*): He-Ne

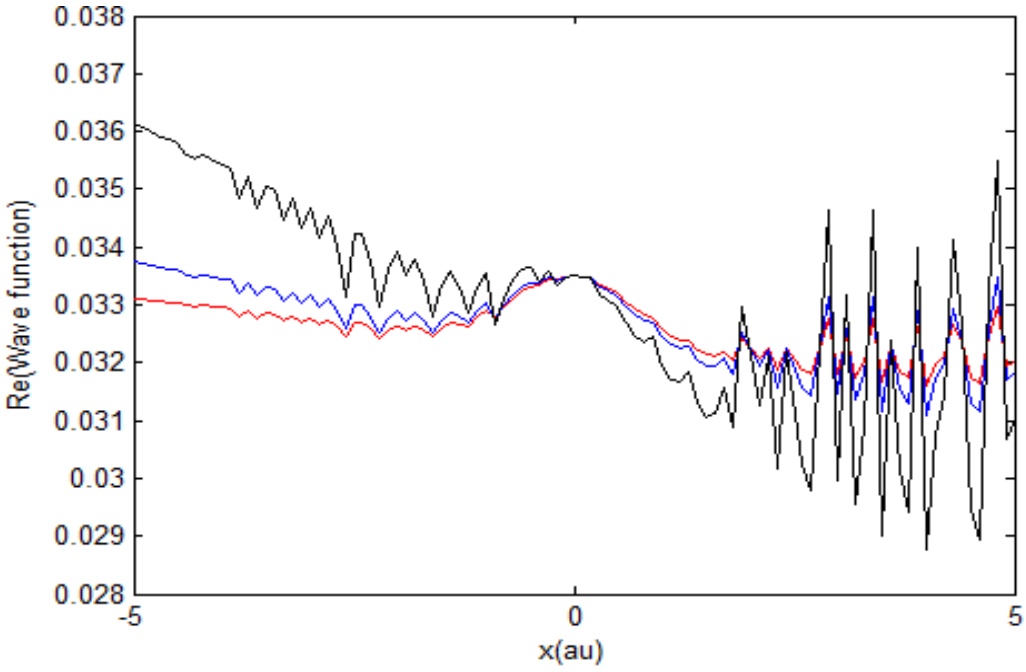

5(c): Ti-Sapphire

Figure 5(b,c). Wave functions for cosine laser electric field with different intensities $1.6\times10^{18}\,\mathrm{Wm}^{-2}$ (red), $5\times10^{18}\,\mathrm{Wm}^{-2}$ (blue) and $40\times10^{18}\,\mathrm{Wm}^{-2}$ (black) for (*b*) He-Ne and (*c*) Ti-Sapphire.

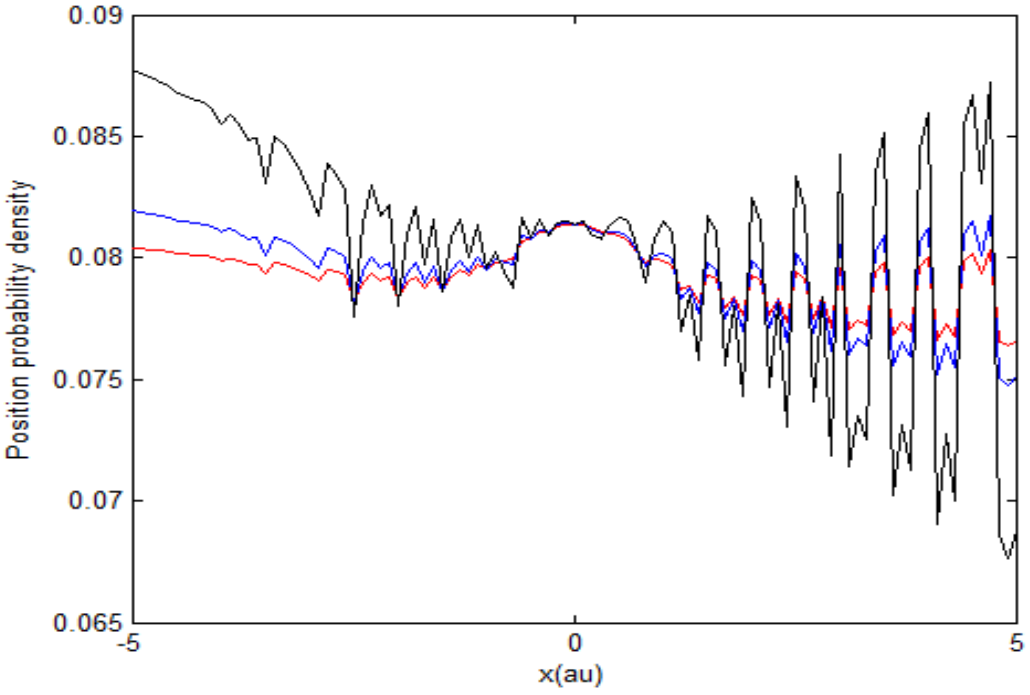
0.09
0.085
0.08
0.075
0.07
0.065
Position probability density
-5
0
5
x(au)

6(*a*): Ar

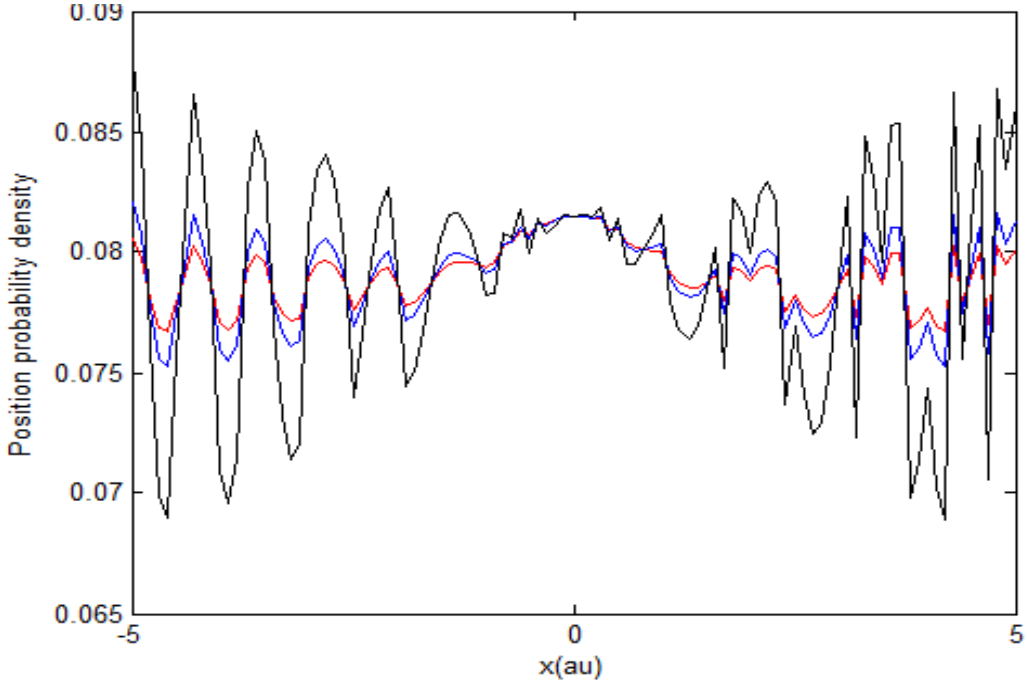
0.09
0.085
0.08
0.075
0.07
0.065
Position probability density
-5
0
5
x(au)

6(*b*): He-Ne

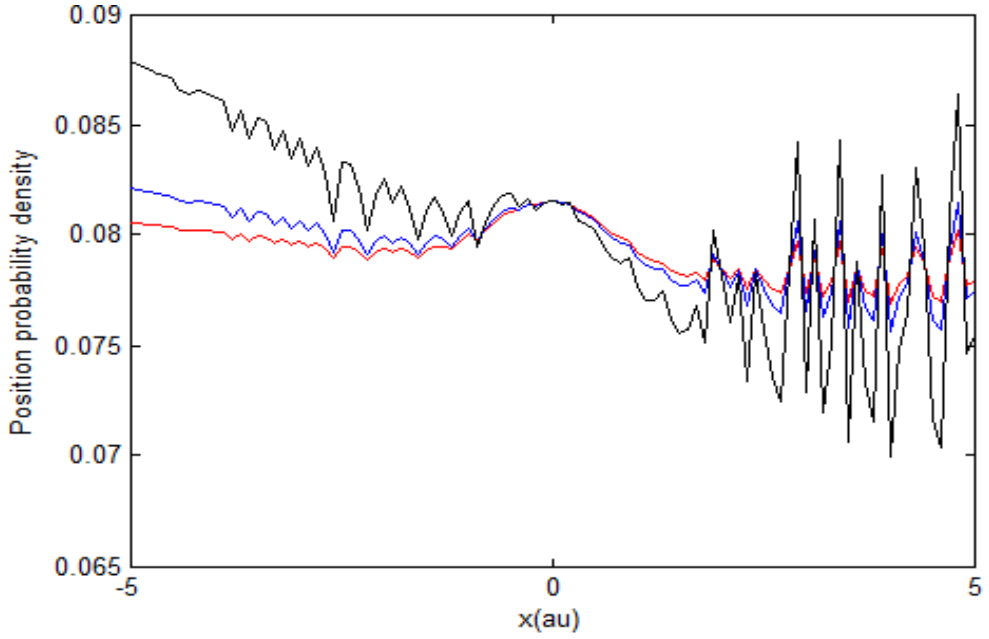

6(c): Ti-Sapphire

Figure 6. Position probability density for (*a*) Ar, (*b*) He-Ne and (*c*) Ti-Sapphire laser field with different intensities $1.6\times10^{18}\,\mathrm{Wm}^{-2}$ (red), $5\times10^{18}\,\mathrm{Wm}^{-2}$ (blue) and $40\times10^{18}\,\mathrm{Wm}^{-2}$ (black) for cosine laser electric field.

The wave function and the position probability density of the Ar, He-Ne and Ti-Sapphire laser fields with different intensities for the cosine electric field is shown in Figure 5 and 6 respectively. Red, blue and black colour lines represents laser field intensity of 1.6×10^{18}, 5×10^{18} and $40\times10^{18}\ \mathrm{Wm}^{-2}$.

As the intensity of the laser increases, the position probability of the electron away from the atom also increases. Most importantly, the wave function distribution is not symmetric and has different patterns along the positive x-axis and negative x-axis for all the three lasers. Therefore the intensity increment will change the position probability density of the electron and there is no symmetry around the atom. A completely different wave function, from Ar laser occurs for the He-Ne laser with cosine electric field. Several peaks can be seen along the positive x-axis and negative x-axis as well. When the intensity is increasing, for Ti-Sapphire laser there is a higher probability for the electron to be along the negative x-axis. The wavelength increment has made the wave functions unique for each plot.

4. SINE LASER ELECTRIC FIELD

The distortions of the atomic potential due to the presence of a strong Ar laser with a sine electric with different intensities are shown in Figure 7. Black colour data points represent the Gaussian potential well without an external laser field. Blue, red and green lines

represent the distorted Gaussian potential after applying the Ar laser intensity of $40\times10^{18}\,\mathrm{Wm^{-2}}$, $5\times10^{18}\,\mathrm{Wm^{-2}}$ and $1.6\times10^{18}\,\mathrm{Wm^{-2}}$ respectively. As the laser intensity increases, the tunnelling probability increases. The barrier potential reduction for sine electric field occurs in the opposite direction to that of cosine electric field. Figure 8 shows the distortion of the Gaussian potential due three different lasers, Ar laser λ = 500 nm in green, He-Ne laser λ = 632.8 nm in red and Ti-sapphire laser λ = 800 nm in blue with sine electric field intensity of $5\times10^{18}\,\mathrm{Wm^{-2}}$. Black colour data points represent the Gaussian potential well without an external laser field. The Gaussian barrier is reduced in the positive direction of x axis for all the three different lasers and when the laser wavelength is increasing, the barrier reduction also is increased.

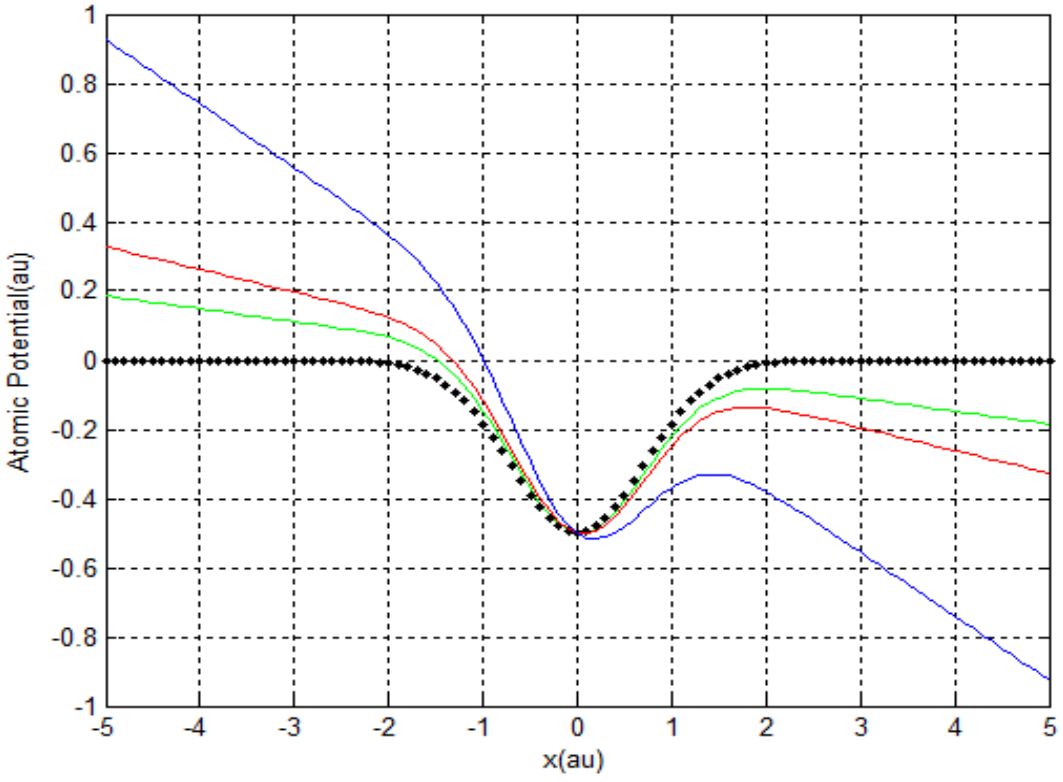

Figure 7. Atomic potential distortion due to the Ar laser field with different intensities (sine electric field) Blue, red and green lines represent intensity $40\times10^{18}\,\mathrm{Wm^{-2}}$, $5\times10^{18}\,\mathrm{Wm^{-2}}$ and $1.6\times10^{18}\,\mathrm{Wm^{-2}}$.

The wave function and the position probability density of the Ar, He-Ne and Ti-Sapphire laser fields with different intensities for the sine electric field is shown in Figure 9 and 10 respectively. Red, blue and black colour lines represents laser field intensity of $1.6\times10^{18}\,\mathrm{Wm^{-2}}$, $5\times10^{18}\,\mathrm{Wm^{-2}}$ and $40\times10^{18}\,\mathrm{Wm^{-2}}$. For different wavelengths, the wave functions and the probability densities are different.

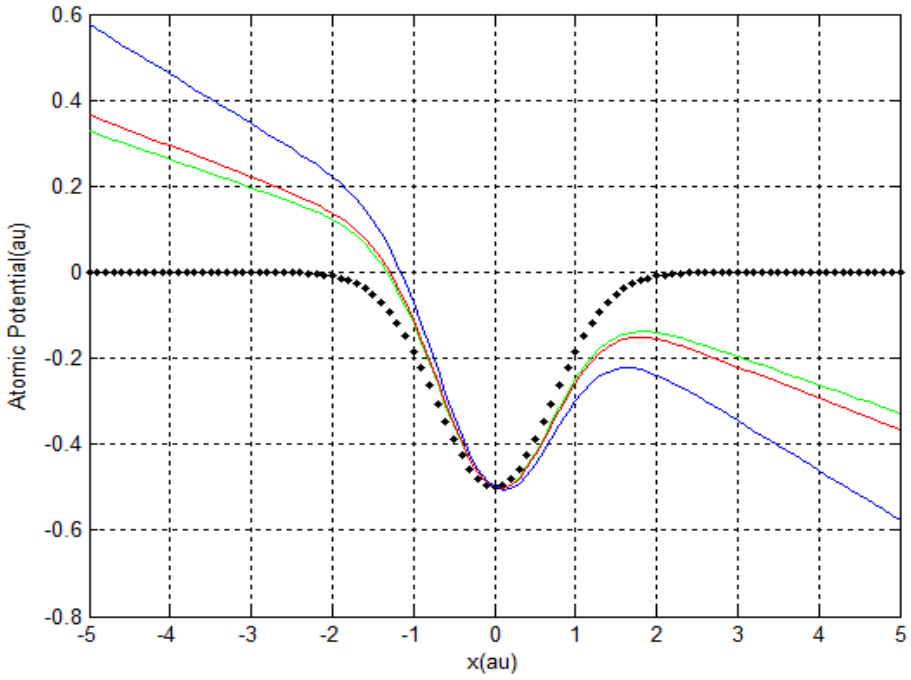

Figure 8. Atomic potential distortion due to sine electric field intensity of $5\times10^{18}\,\mathrm{Wm}^{-2}$. Green red and blue, lines represent Ar, He-Ne and Ti-sapphire laser. Black lines are without an external laser field.

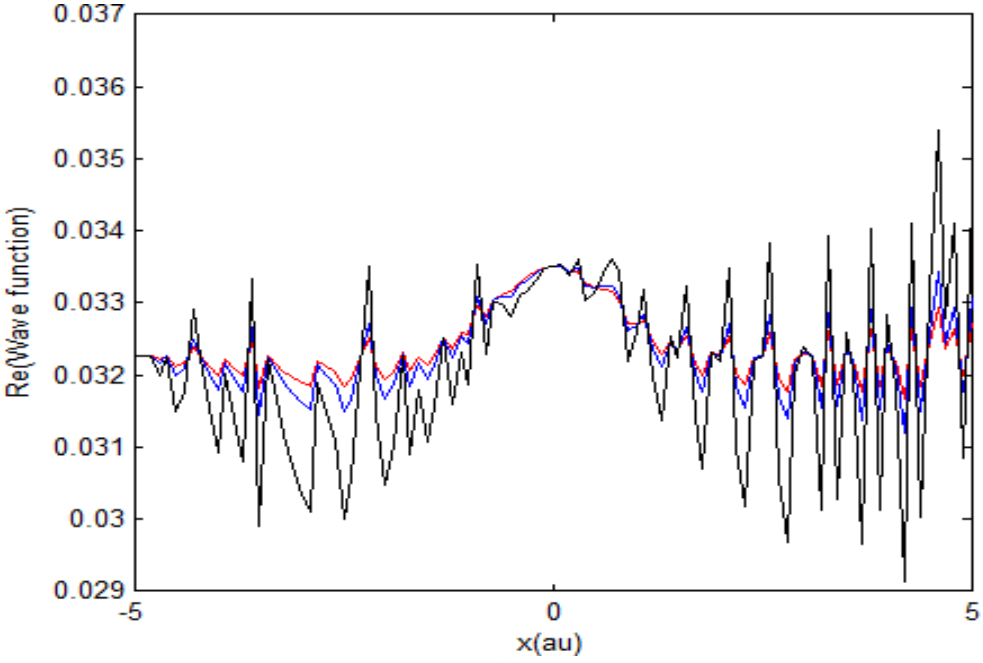

9(*a*)

Figure 9(*a*). Wave function for Ar, sine laser electric field with different intensities $1.6\times10^{18}\,\mathrm{Wm}^{-2}$ (red), $5\times10^{18}\,\mathrm{Wm}^{-2}$ (blue) and $40\times10^{18}\,\mathrm{Wm}^{-2}$ (black) for.

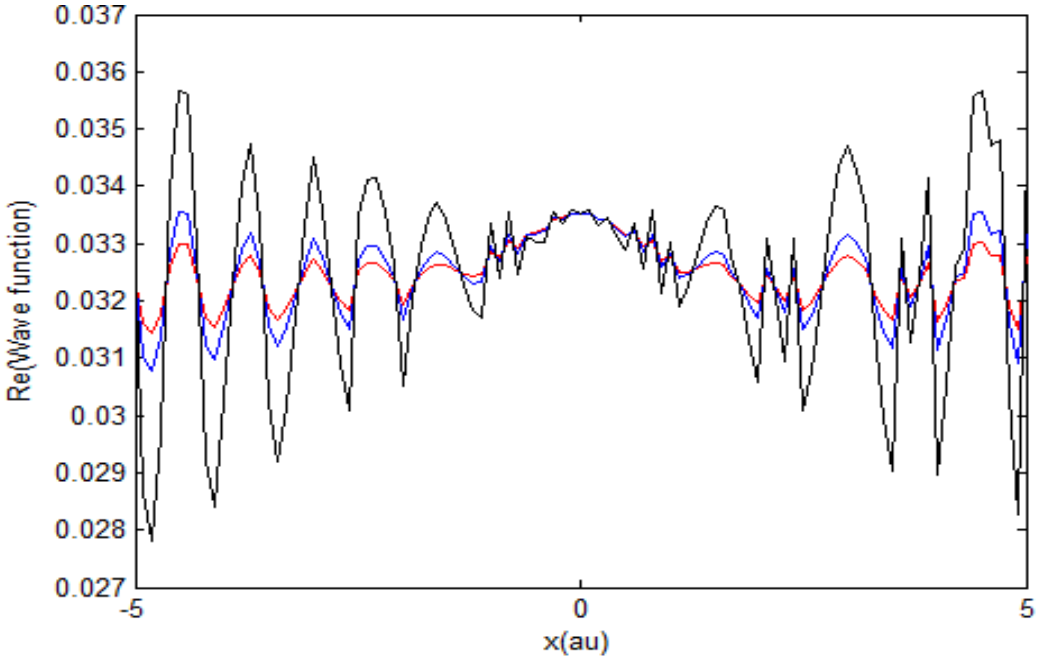

9(*b*): He-Ne

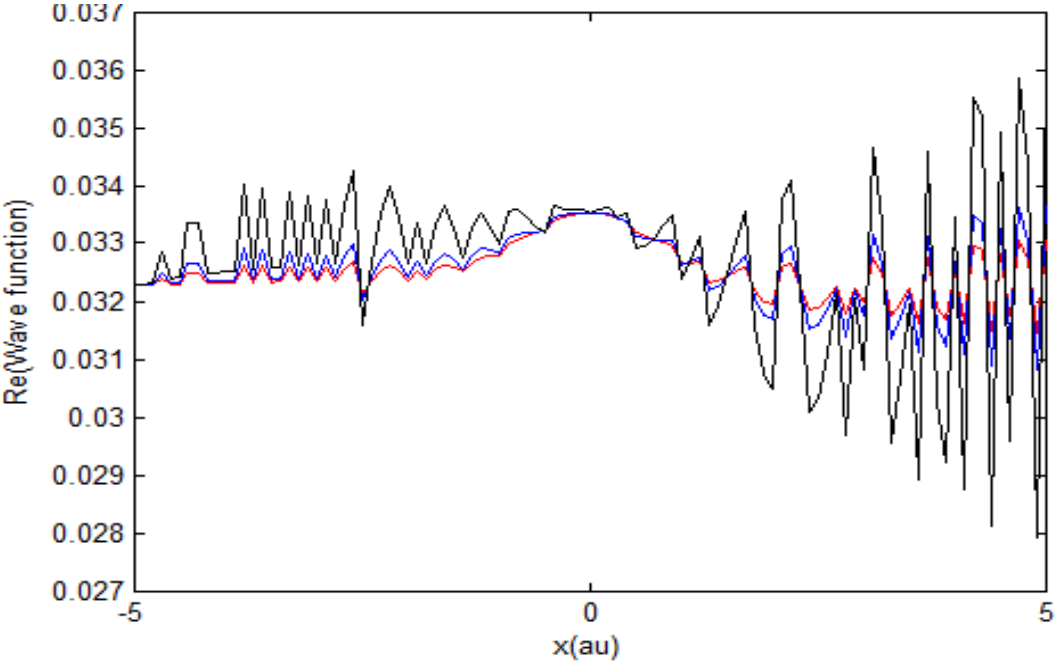

9(*c*): Ti-Sapphire

Figure 9(b,c). Wave functions for (*b*) He-Ne and (*c*) Ti-Sapphire laser field with different intensities $1.6\times10^{18}\,\mathrm{Wm}^{-2}$ (red), $5\times10^{18}\,\mathrm{Wm}^{-2}$ (blue) and $40\times10^{18}\,\mathrm{Wm}^{-2}$ (black) for sine laser electric field.

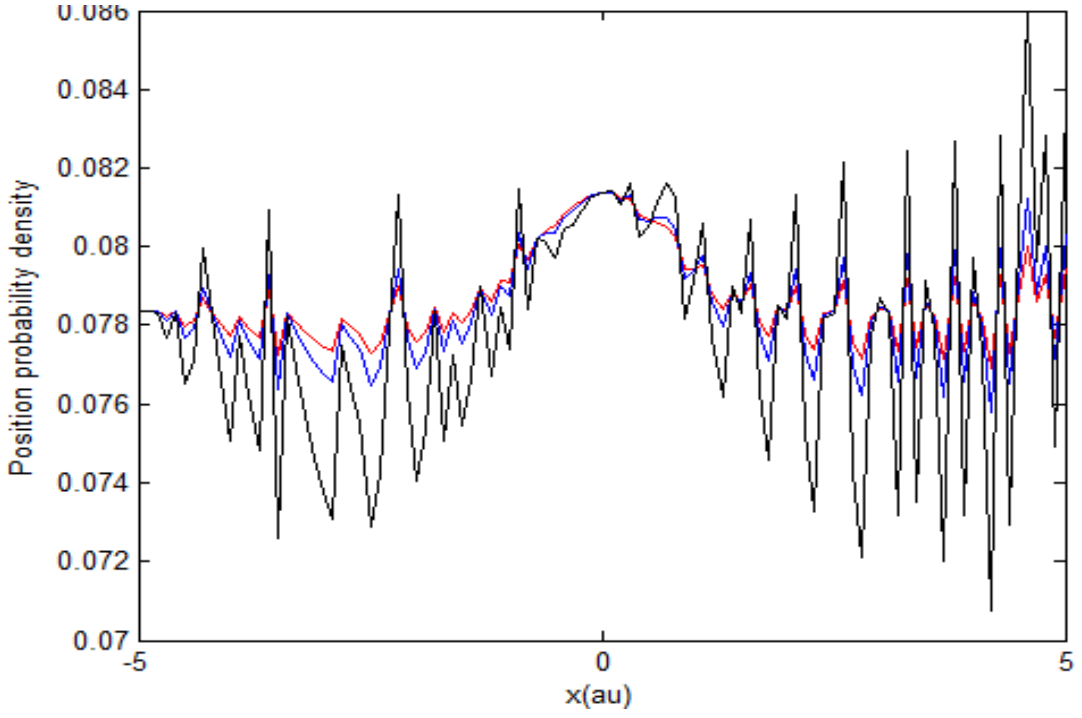
0.086
0.084
0.082
0.08
0.078
0.076
0.074
0.072
0.07
Position probability density
-5
0
5
x(au)

10(*a*)

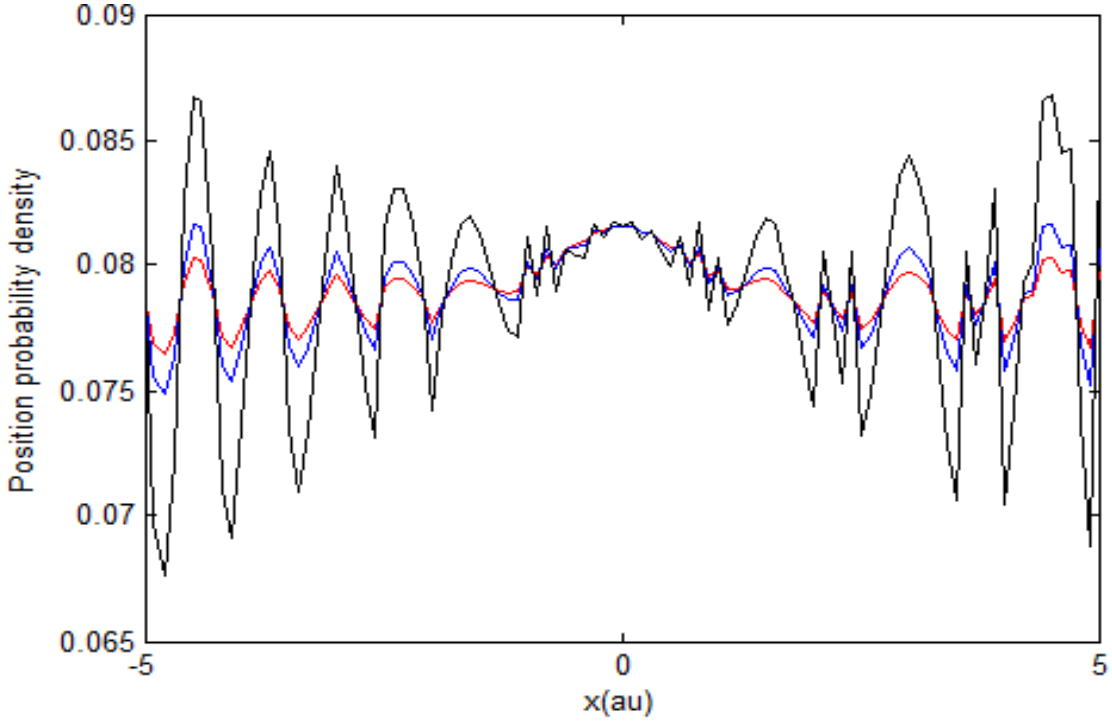
0.09
0.085
0.08
0.075
0.07
0.065
Position probability density
-5
0
5
x(au)

10(*b*)

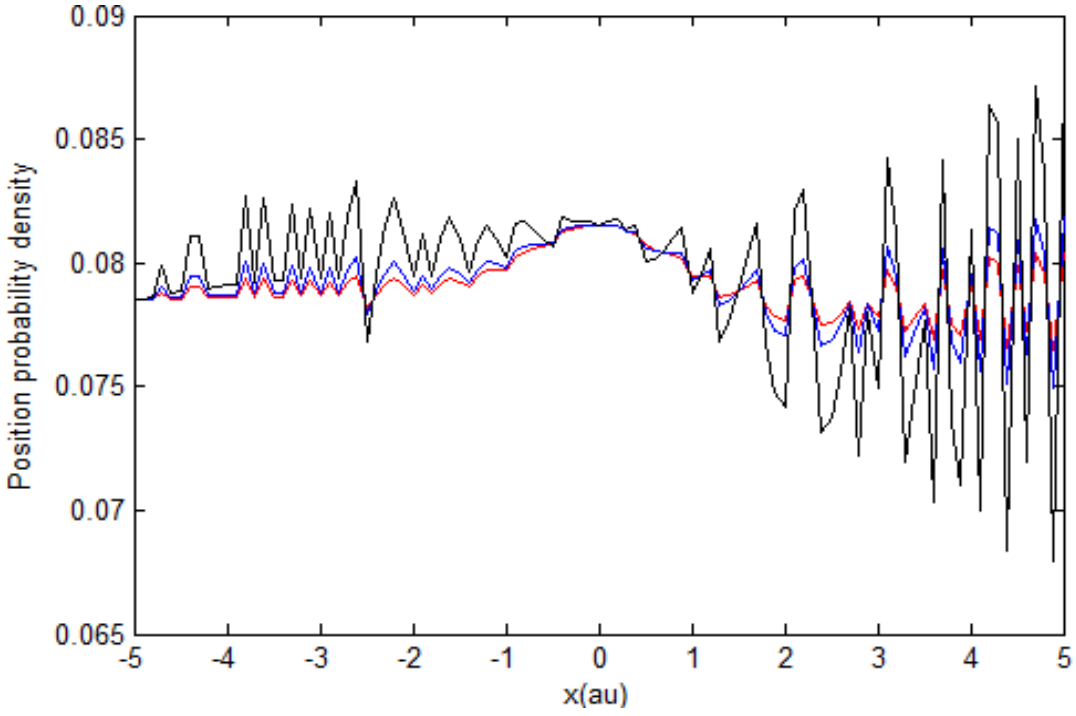

10(c)

Figure 10(a-c). Position probability density for (*a*) Ar, (*b*) He-Ne and (*c*) Ti-Sapphire sine laser electric field intensities $1.6\times10^{18}\,\mathrm{Wm}^{-2}$ (red), $5\times10^{18}\,\mathrm{Wm}^{-2}$ (blue) and $40\times10^{18}\,\mathrm{Wm}^{-2}$ (black)

5. TWO DIMENSIONAL GAUSSIAN WELL

The time dependent Schrodinger equation in two dimensions with an external laser field applied in the x direction, can be written as:

$$\left[\frac{-\hbar^2}{2m}\left(\frac{\partial^2}{\partial x^2}+\frac{\partial^2}{\partial y^2}\right)+V(x,y)+xE(t)\right]\Psi(x,y,t) = i\hbar\frac{\partial\Psi(x,y,t)}{\partial t} \quad (5)$$

With the atomic Gaussian potential well given in equation 2 equation 5 was solved using Split step method for the wave function of the Gaussian potential well,

$$\Psi(x,y,t) = \left(\frac{2b}{\pi}\right)^{\frac{1}{4}} e^{-b\left(x^2+y^2\right)} e^{\frac{-iEt}{\hbar}} \quad (6)$$

b is related to the width of the potential well and the energy eigenvalue *E* is given by

$$E = \frac{-\hbar^2}{2m}\left(-4b + 4b^2x^2 + 4b^2y^2\right) + V_0(x,y) \quad (7)$$

The simulations were done using the Ar laser with 500 nm wavelength and with the intensity of $5\times10^{18}\,\mathrm{Wm}^{-2}$.

The ionization energy of the ground state electron was chosen as the depth of the Gaussian potential well and values were measured in atomic units. Ionization energy of 13.6 eV used in atomic units to do the simulations for a single electron process.

Figure 11 shows the Gaussian potential well used for the simulation. Atomic potential distortions due to the Ar laser with cosine and sine electric field with different intensities are shown in figure 12. Black colour data points represent the Gaussian potential well without an external laser field.

Blue, red and green lines represent the distorted Gaussian potential well after applying the Ar laser intensity of $40\times10^{18}\,\mathrm{Wm}^{-2}$, $5\times10^{18}\,\mathrm{Wm}^{-2}$ and $1.6\times10^{18}\,\mathrm{Wm}^{-2}$ respectively. As the laser intensity is increases, the tunnelling probability increases.

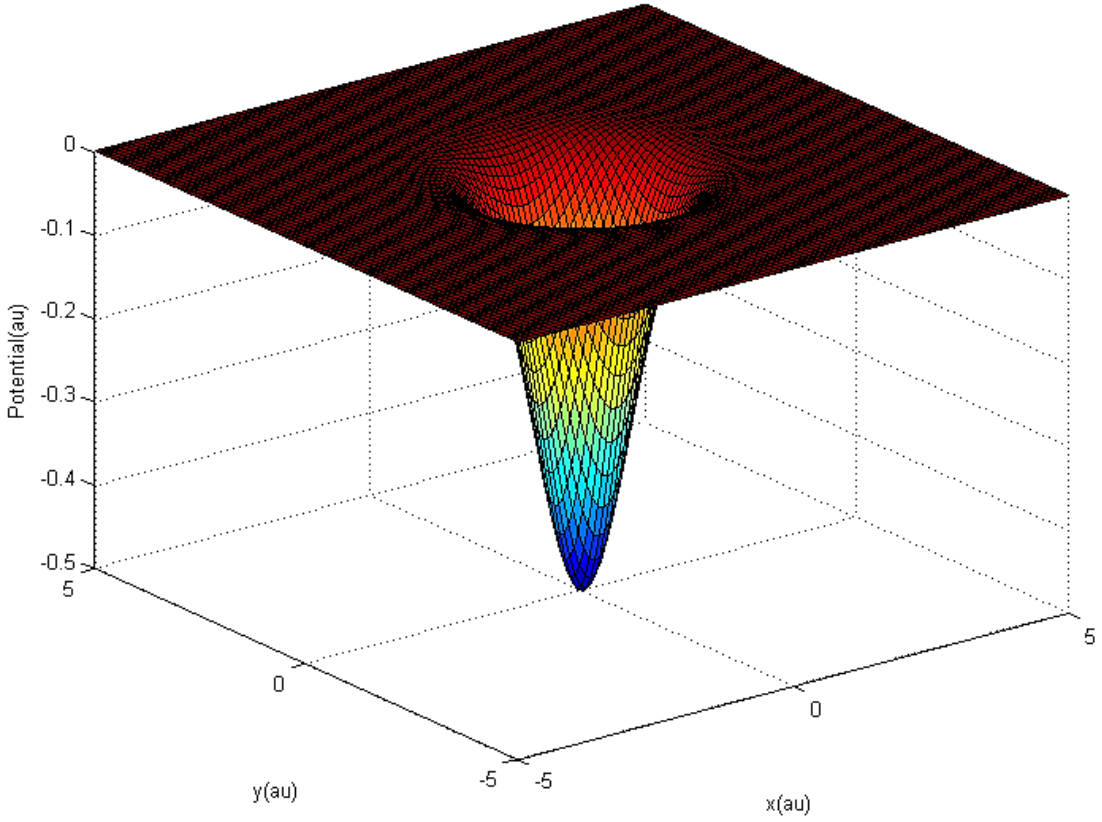

Figure 11. Gaussian potential well used for simulation.

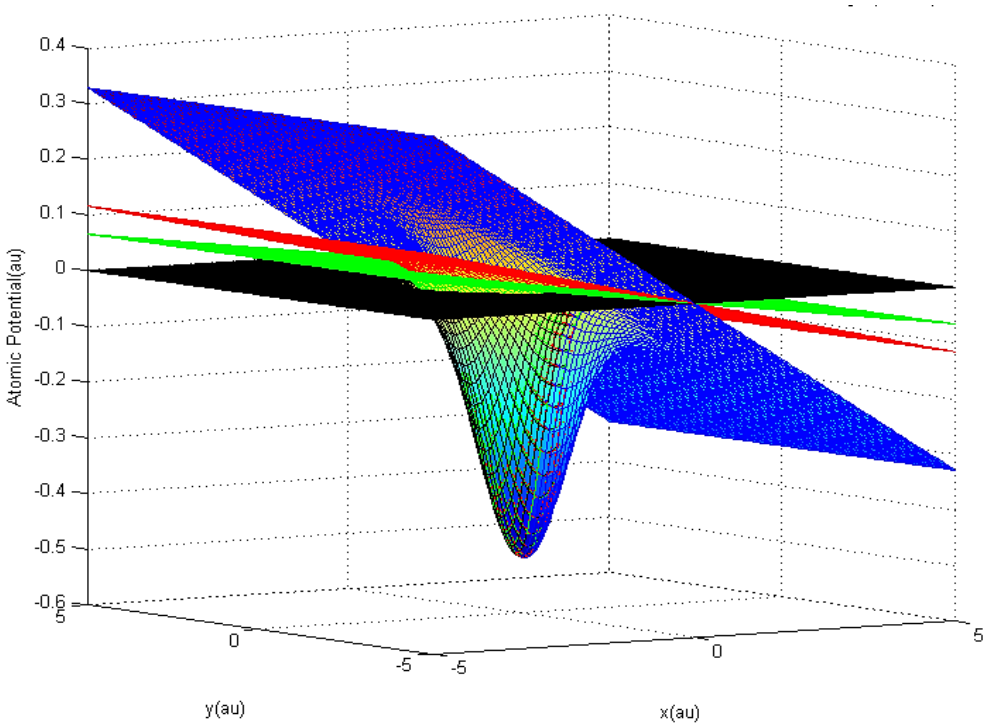

12(*a*)

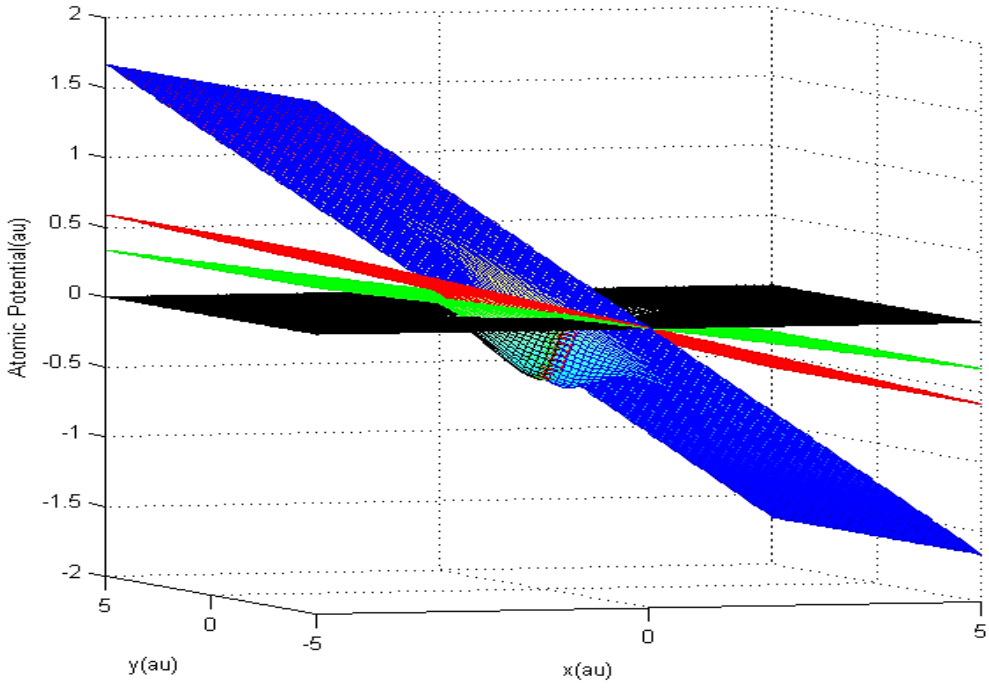

12(*b*)

Figure 12(a,b). Atomic potential distortion due to the Ar laser field with different intensities for (a) cosine and (b) sine electric field. Black colour data points represent the Gaussian potential well without an external laser field and blue, red and green lines represent the distorted Gaussian potential well after applying the Ar laser intensity of 40×10^{18} Wm^{-2}, 5×10^{18} Wm^{-2} and 1.6×10^{18} Wm^{-}

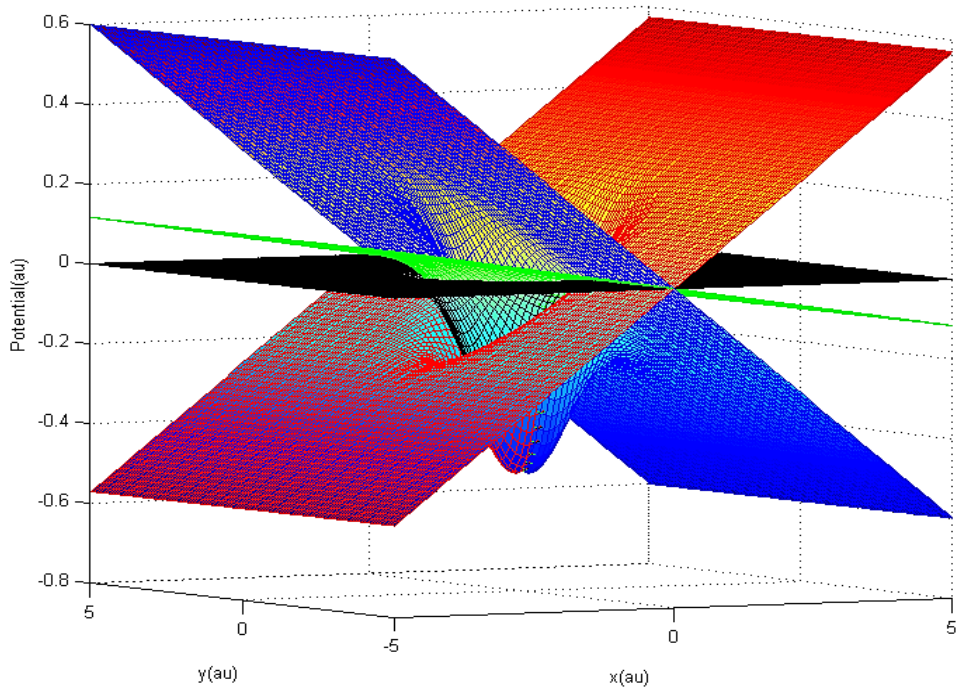

13(*a*)

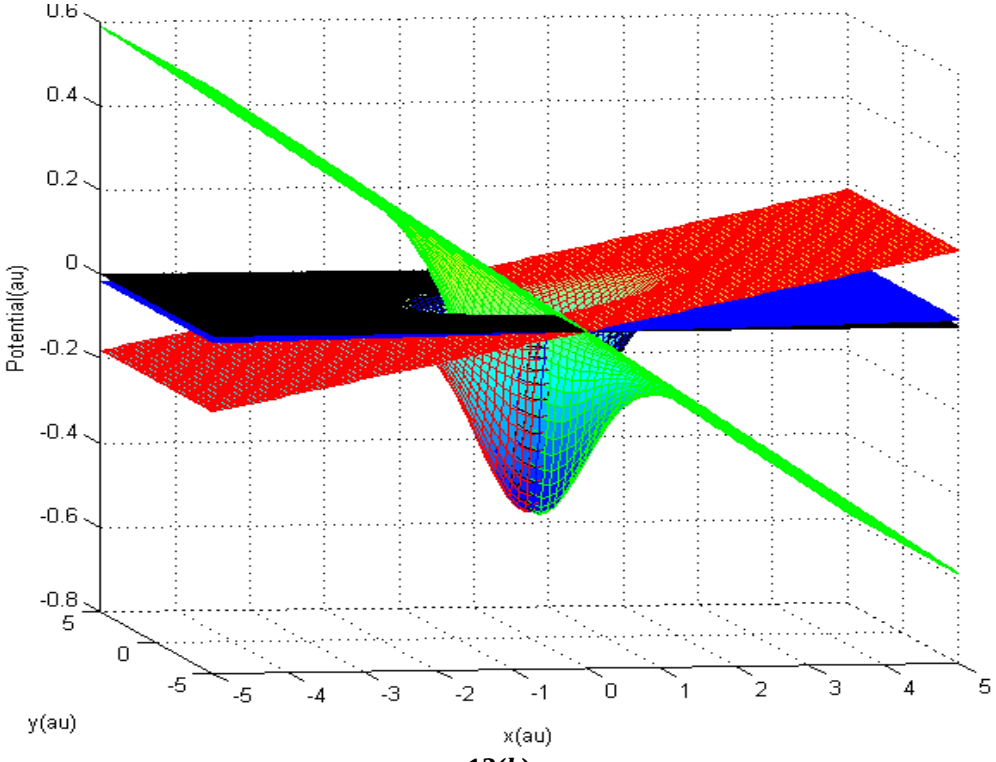

13(*b*)

Figure 13(a,b). Atomic potential distortion due to (*a*) cosine (*b*) sine electric field intensity of $5\times10^{18}\,\mathrm{Wm}^{-2}$. Green, red and blue lines represent Ar, He-Ne and Ti-sapphire laser. Black lines are without an external laser field.

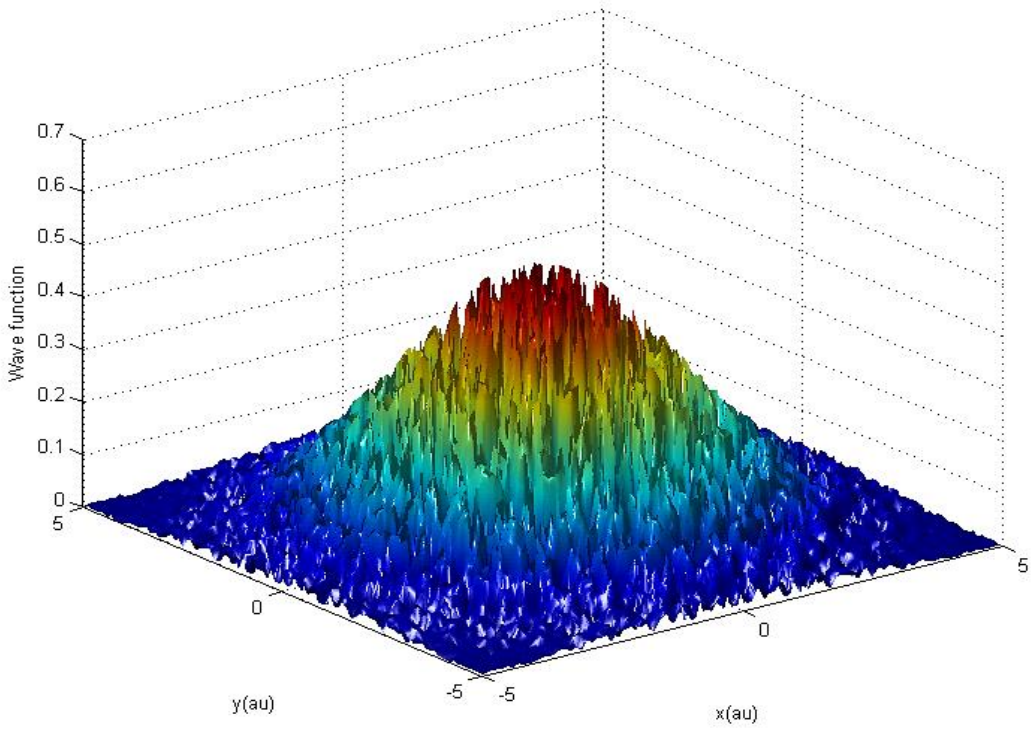

14(*a*)

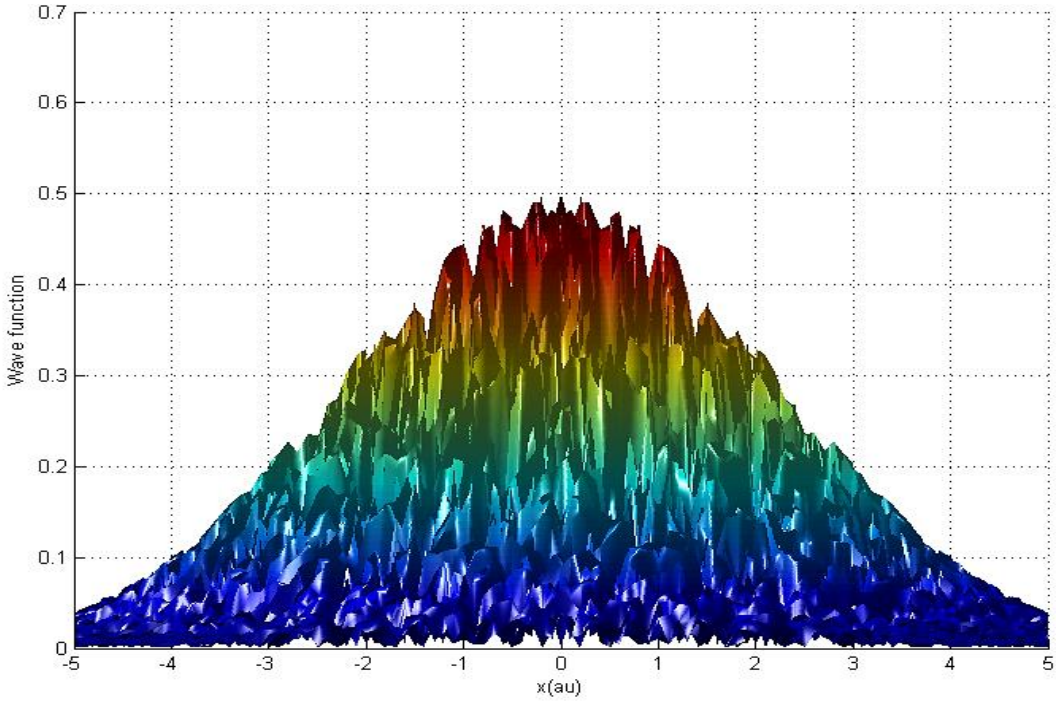

14(*b*)

Figure 14(a,b). Wave function of the electron using the 2D Gaussian potential well with the Ar laser with (*a*) cosine and (b) sine electric field with the intensity of 5×10^{18} Wm^{-2}

The distortion of the Gaussian potential due three different lasers, Ar laser λ = 500 nm in green, He-Ne laser λ = 632.8 nm in red and Ti-Sapphire laser λ = 800 nm in blue with cosine and sine electric field intensity of $5\times10^{18}\,\mathrm{Wm}^{-2}$ are shown in Figure 13. Black colour data points represent the Gaussian potential well without an external laser field. For the cosine electric field, the Gaussian barrier is reduced in the positive direction of x axis for Ar laser and Ti-Sapphire laser, but for the He-Ne laser, the Gaussian barrier reduction occurs in the negative direction of the x axis. In the case of sine electric field, the Gaussian barrier is reduced in the negative direction of x axis for He-Ne laser and Ti-Sapphire laser but for the Ar laser, the Gaussian barrier reduction occurs in the positive direction of the x axis.

The wave function of the electron using the two dimensional Gaussian potential well with the Ar laser λ = 500 nm with cosine and sine electric fields with the intensity of $5\times10^{18}\,\mathrm{Wm}^{-2}$ is shown in figure 14. The wave function does not have a symmetric shape, but the position probability density is higher around the centre of the x and y axis.

6. CONCLUSIONS

With the strong laser field the Gaussian potential well get distorted completely removing the symmetric shape of the potential well. The distortion of the Gaussian potential well changes with the laser intensity and laser wavelength. He-Ne laser with the wavelength of 632.8 nm has a totally opposite impact on the potential well compared to the Ar and Ti-sapphire lasers for the one dimensional potential well with cosine electric field. The wave functions are different for the laser field with the cosine electric field and sine electric field. The wavelength of the laser has an impact on the wave function as well. Furthermore, for the He-Ne laser the wave functions have similar patterns with the cosine and sine electric fields. For the three different lasers, the wave functions are not symmetric about the parent atom and as the intensity increases the probability densities away from the parental atom increases. The wave function due to the strong field laser applied to the two dimensional atomic potential shows that there is a higher probability density near the centre of the x axis and y axis. The wave functions complexity is mostly accompanied with the higher frequency value and finally, the laser characteristics have an effect on the behaviour of the electron which tunnels through the potential barrier.

References

[1] K. Jakubczak, Laser Pulse Phenomena and Applications: *High-order Harmonic Generation*, edited by F.J. Durate (InTech, 2010) 4-79 www.intechopen.com

[2] A. L'Huillier, *Europhysics news*, 33(6) (2002) 205-207.

[3] M.F. Kling, M.J.J. Vrakking, Attosecond electron dynamics. *Annu. Rev.Phy.Chem.* 59 (2008) 463-92.

[4] K.L. Ishikawa, Advances in Solid-State Lasers: Development and Applications, chapter 19: *High-Harmonic Generation* Edited by Mikhail Grishin (InTech, 2010) 439-464.

[5] T. Matthey, T.Sørevik, Solving the 3d time dependent Schrödinger equation by a parallel split-step spectral method, *Parallel Computing: Software Technology, Algorithms, Architectures, and Applications Proceedings of the 10th ParCo Conference in Dresden*, 2(3) (2003) 3-8.

[6] C.C. Gunatilaka, K. A. I. L. Wijewardena Gamalath, *World Scientific News* 35 (2016) 1-16.

[7] S. Nandi, *American Journal of Physics*, 78 (12) (2010) 1341-1345.

(Received 30 January 2016; accepted 10 February 2016)